Dry Metal Forming Open Access Journal

Fast Manuscript Track

Edited by Frank Vollertsen
Available online at https://elib.suub.uni-bremen.de/

www.drymetalforming.de

Dry Met. Forming OAJ FMT 5 (2019) 025–030
Received Nov 15, 2019; published Nov 26, 2019

Friction reduction in dry forming by using tetrahedral amorphous carbon coatings and laser micro-structuring

Theresa Jähnig*[1], Ali Mousavi[1], Maximilian Steinhorst[1,2], Teja, Roch[2], Alexander Brosius[1], Andrés Fabián Lasagni[1,3]

[1] Institute for Manufacturing Technology, Technische Universität Dresden, 01062 Dresden
[2] Fraunhofer IWS, Institute for Material and Beam Technology, Eberhardstraße 12, 44145 Dortmund
[3] Fraunhofer IWS, Institute for Material and Beam Technology, Winterbergstraße 28, 01277 Dresden

Abstract

Friction has a dominant influence on manufacturing processes. In deep drawing of sheet metals, lubricants are regularly used to reduce friction forces. However, significant production costs originate from their supply, application, removal and disposal. The negative environmental consequences of using lubricants promote extended research on lubricant free deep drawing processes and tools. A combination of macro-structuring in the flange area and micro-structuring of ta-C layers at the pulling edge radius of deep drawing tools is identified to compensate the loss of tribological functions. Surface texturing of semi-finished sheet metals also supports friction reduction by minimizing the contact area to the deep drawing tool. In this study, a variation of ta-C coating iterations with several coating and decoating steps, as well as microstructuring of the ta-C coatings using Direct Laser Interference Patterning was used on cylinders in draw bend test rigs. The resulting friction coefficients between the cylinders and steel stripes show minimal friction for ta-C covered draw bend tools.

Keywords: ta-C coating, direct laser interference patterning, friction reduction, dry forming, lubricant free forming

1 Introduction

Forming processes, especially deep drawing processes, take advantage of the use of additional lubricants to reduce the interfacial forces between tool and work piece. Thus, friction and wear must be significantly decreased to allow the improvement of the tool lifetime as well as an enhanced surface finish of the produced products.

As the lubricants typically remain on the tool and work piece after the forming process, the necessity of additional cleaning procedures is given, including the environmental and economic issues with the lubricant handling and disposal [1]. In consequence, concepts based on lubricant free forming – namely dry forming – come in the last years into focus, such as the application of protective coatings [2-6].

In this work, an optimization of the tool design for deep drawing applications is suggested by employing functional coatings in combination with a micro-structuring to control friction, wear and material flow. As protective coating, a layer of tetrahedral amorphous carbon (ta-C) is applied which combines a low friction coefficient with a high hardness and wear resistance [7-11]. The ta-C coating is capable of taking over the tribological functions of the lubricant while protecting the microstructures [12].

The process of micro-structuring is performed using Direct Laser Interference Patterning (DLIP) to add further modification of the tribological performance, e.g. by reducing the interfacial contact area and providing wear particle traps [13, 14]. DLIP enables the fabrication of periodic surface structures on different material surfaces by transferring the shape of interference patterns directly to the treated materials. The periodic patterns are produced in one step, without the necessity of ensuing wet chemical [15, 16] or imprinting steps. In DLIP, a pulsed laser beam is split into several partial beams and recombined on the material surface (Fig. 1). The geometry of the obtained spatial energy distribution depends on the number of sub-beams, the used wavelength λ and the angle θ between beams[17-19]. In addition, the spatial period p, defined as the distance between two intensity maxima (or minima) can be calculated for a two-beam configuration using Eq. 1:

*E-mail address of corresponding author: theresa.jaehnig@tu-dresden.de

$$p = \frac{\lambda}{2\sin(\theta)} \quad (1)$$

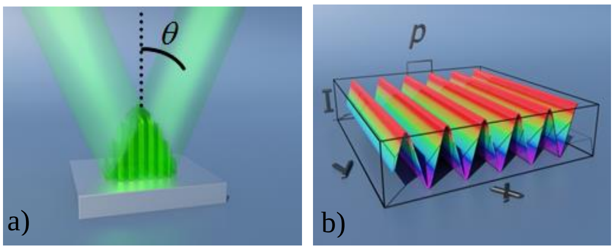

Fig. 1: a) Overlap of two sub-beams on the sample surface with angle $\boldsymbol{\theta}$. b) Spatial distribution of the intensity maxima (or minima) in x – and y- direction, with period p.

In addition to the laser texturing process, also a variety of ta-C coating procedures, including decoating steps or the use of process gas during the deposition is also investigated and tested in draw bend tests. Combined with the DLIP micro-structuring of the coated cylinders, their tribological properties and long-term stability were investigated.

2 Results and Discussion

2.1 Plasma surface preparation

The cylinders were thoroughly cleaned with methanol, distilled water and dried with nitrogen before putting them on holders. Certain cylinders were nitrided by a plasma enhanced CVD process before they were coated with a ta-C layer. Therefore, a PC 100/150-S system from Rübig GmbH and as process gas a mixture of 80 % N_2 and 20 % H_2 were used. The chamber was evacuated to a base pressure of approximately 200 Pa and heated up to 550 °C.

The ta-C coatings were deposited by the short pulsed arc technique (spArc®, Inovap C57T PVD system). A continuous DC-arc is superimposed by a short high-current pulse with a frequency of 100 Hz, pulse duration up to 300 µs and a current of about 1500 A. Due to this superimposition, a significant increase of the ion energy is achieved leading to a great densification. Thus, the resulting films exhibit a high degree of sp^3-bonded carbon atoms. The vacuum chamber was evacuated to a base pressure between 10^{-3} and 10^{-5} Pa using a rotary and a turbo molecular pump. In order to remove the native oxide layer and to clean the cylinders were sputtered with metal ions. For an improved adhesion between the coating and the substrate, a metallic interlayer was deposited at temperatures above 100 °C by applying a low-voltage bias.

Pure graphite targets (99.99 %) were used for ta-C coatings. The deposition of the ta-C coating is divided in two steps. At first, an implantation process was conducted followed by the deposition of the carbon thin films at temperatures below 100 °C using the spArc technique.

It is known that the properties of ta-C can be modified by using a process gas during the deposition [20, 21]. In order to evaluate the effect of the process gas on the friction coefficient, additional samples were coated with ta-C in N_2-atmosphere. This was performed by introducing 15 sccm of N_2 into the chamber during the deposition of the ta-C coating without adjusting the other process parameters. Some of the coated cylinders were decoated by the tampon method using a two-electrode setup, including a rod-shaped graphite cathode (Fig. 2).

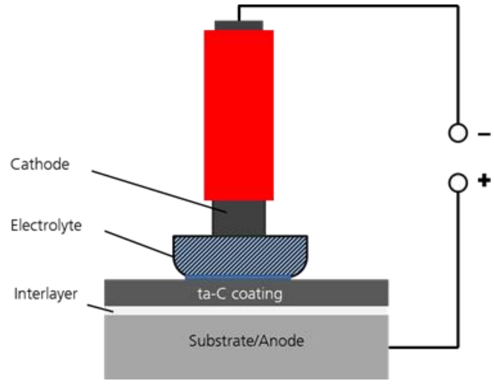

Fig. 2: Scheme of the tampon method setup. Around the cathode rod a cotton pad soaked with the electrolyte is attached. By scrubbing the tampon over the surface and applying a voltage between the cathode and the substrate an electrochemical reaction occurs.

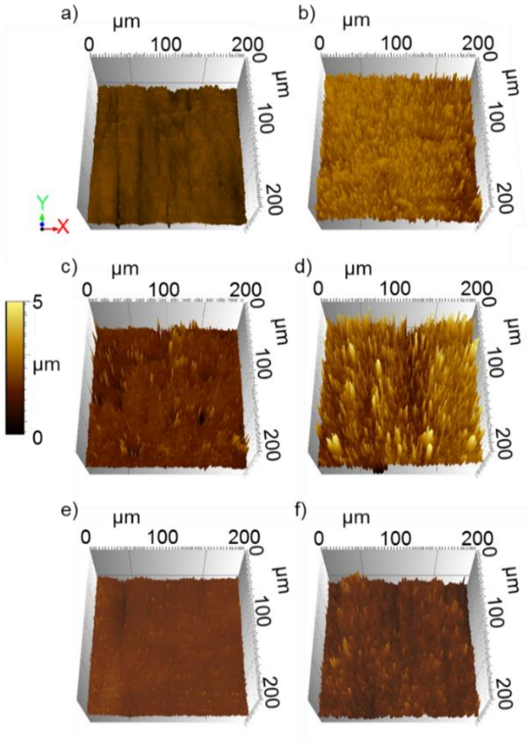

Fig. 3: Confocal microscope images of the differently prepared cylinder surfaces: uncoated, polished reference a), ta-C coated b), ta-C coated and decoated c), ta-C coated, decoated and ta-C coated d), nitrided and ta-C coated e) and ta-C coated in N_2-atmosphere f).

A cotton pad soaked was attached to the cathode in a sodium hydroxide solution serving as the electrolyte. By applying a constant voltage of 10 V (Selectron SPS-1560-AH) and scrubbing the cathode over the sample surface an electrochemical reaction occurs which leads to the removal of the coating. Confocal microscope images of the different prepared surfaces are shown in Fig. 3. Also, values for surface roughness and layer thickness are given in Table 1.

Table 1: Roughness and thickness of the deposit layers on the prepared cylinder surfaces

Sample	Sa [µm]	Sz [µm]	Sq [µm]	Layer thickness [µm]
uncoated	0.062 ± 0.009	0.963 ± 0.058	0.079 ± 0.011	-
ta-C coated	0.243 ± 0.007	3.975 ± 0.435	0.359 ± 0.024	6.95
ta-C coated + decoated	0.615 ± 0.062	9.500 ± 0.571	0.822 ± 0.058	-
ta-C coated + decoated + ta-C coated	0.427 ± 0.008	6.940 ± 0.099	0.616 ± 0.008	4.78
nitrided + ta-C coated	0.122 ± 0.008	3.680 ± 1.032	0.164 ± 0.014	3.79
ta-C coated in N_2-atmosphere	0.240 ± 0.019	3.790 ± 0.227	0.321 ± 0.026	3.63

2.2 Micro-structuring with Direct Laser Interference Patterning

Using the DLIP technology (see introduction section), different coatings were treated with the aim of producing periodic surface patterns.

The used system utilizes a solid-state Nd:YVO4 laser (Edgewave PX 200) emitting 1064 nm wavelength with 10 ps pulse duration and repetition rates up to 30 kHz and maximum output power of 10 W. The workstation is equipped with a commercial available DLIP optical head (manufactured by Fraunhofer IWS, Germany), which uses a diffractive optical element (DOE) to split the initial laser beam into two sub-beams.

These two beams go through a prism where they are parallelized and then focused on the sample using a 60 mm aspheric lens, obtaining a line-like interference intensity profile at the interference point with 140 µm in diameter. The samples were translated in the x and y - directions by using high-precision axes (Aerotech, USA) with an accuracy of ± 2.5 µm.

For the structuring on the curved surfaces, the DLIP setup has been modified. This modification permitted to treat half-round surfaces. In a first step, the focus distance was measured from the highest position on cylinder surface (Position 1 at Fig. 4a). By moving the DLIP setup along the cylinder radius, the z-axis was programmed to keep the distance between the focus lens of the DLIP head and the sample surface constant. This allowed maintaining the interference volume on the material surface during the structuring process along the cylinder radius. The largest structure heights were measured at position 1, indicated in Fig. 4a) and Fig. 4c), for an inclination angle of 0° of the laser beam with respect to the cylinder's surface. By moving the laser spot along the radius, the inclination angle and the spot size increased, resulting in a decreased laser fluence due to the cylinder curvature. In consequence, the structure heights at position 2 in Fig. 4a) and Fig. 4d) decreased.

For the application of the microstructures on the pulling edge radius of deep forming tools, the DLIP setup was tested with an additional mirror between the last lens of the DLIP head and the curved surface (see Fig. 4b). With this modification, the largest structure heights will be half-way of the pulling edge (position 1 Fig, 4b), where the highest friction is expected.

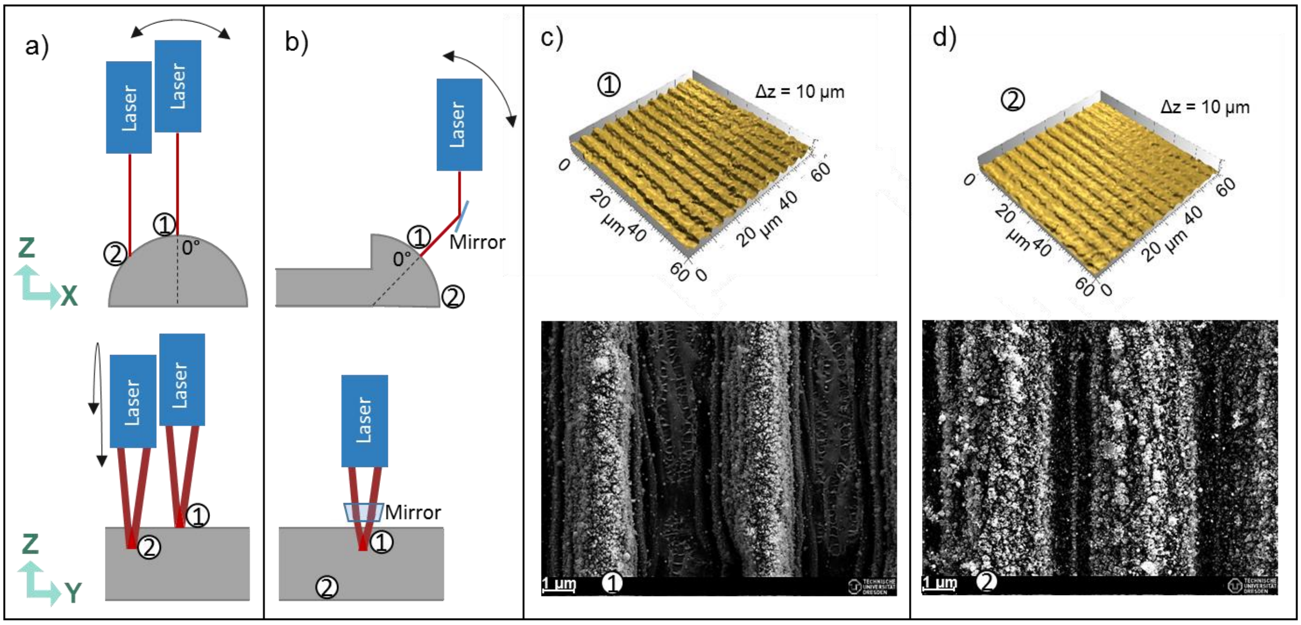

Fig. 4: Standard DLIP setup with vertical laser beam and inclination angle of 0° for structuring of a cylindrical surface a) and a modification of the DLIP setup by placing a mirror between the last lens of the DLIP head and the pulling edge radius of the dry forming tool b). Confocal images and SEM images for surfaces corresponding to position 1 and 2 on the half-round surfaces c) and d) [22].

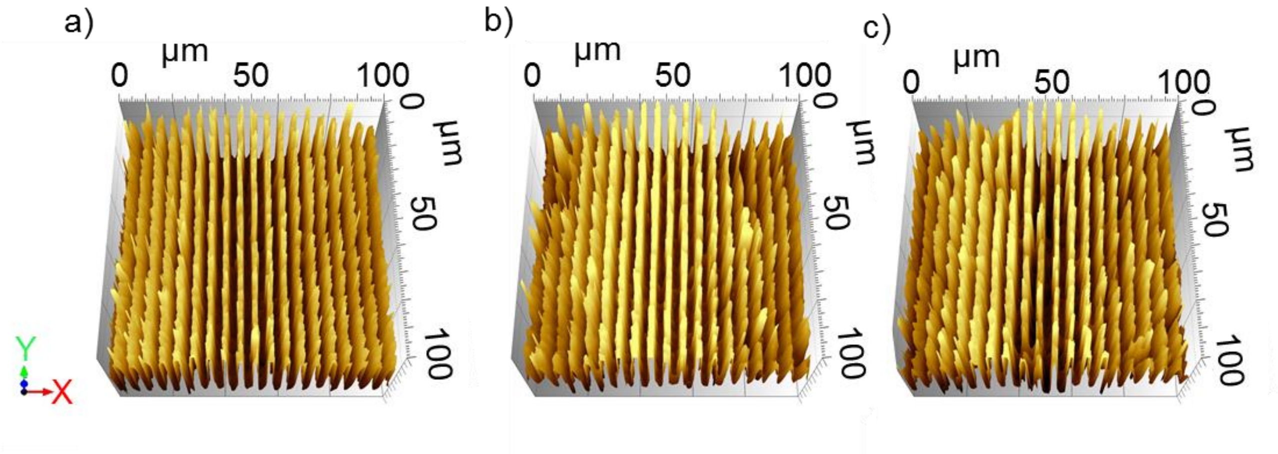

Fig. 5: Confocal microscope images of the DLIP structures on differently prepared cylinder surfaces: a) ta-C coated, b) three times ta-C coated and decoated in between, and c) nitrided and ta-C coated (taken with 150x magnification objective).

The surface roughness and the structure heights, achieved on the differently coated cylinders, can be found in Table 2, measured on position 1 corresponding to Fig. 4a. Corresponding confocal images are shown also in Fig. 5.

Table 2: Roughness and structure heights after the DLIP micro-structuring process.

Sample	Sa [µm]	Sz [µm]	Sq [µm]	Structure height [µm]
ta-C coated + DLIP	1.236 ± 0.264	9.745 ± 0.205	1.155 ± 0.035	3.431 ± 0.448
ta-C coated + decoated + ta-C coated + decoated + ta-C coated + DLIP	0.931 ± 0.004	15.65 ± 0.152	1.234 ± 0.023	3.669 ± 0.345
nitrided + ta-C coated + DLIP	1.471 ± 0.073	8.22 ± 0.024	1.615 ± 0.055	3.565 ± 0.326

2.3 Draw bend test

The tribological tests were performed with a draw bend test machine under 90° deflection (Fig. 6). Commercially-sourced DC04 metal stripes with 1000 mm length, 20 mm width and 1 mm thickness were drawn over the test cylinders, prepared with the different coated and structured surfaces. The initial surface roughness was Sa = 1.21 ± 0.341 µm The drawn bend tests were carried out at room temperature under dry conditions with a constant drawing velocity of 100 mm/s and a contact surface pressure 50 MPa.

For each cylinder variation at least two cylinders were evaluated, each with four untreated DC04 stripes bend over them. The drawn length per stripes was 400 mm, resulting in a 1600 mm length drawn over each cylinder.

The results of the friction coefficient measurement can be found in Fig. 7. The diagram shows the largest friction coefficient for the untreated, unlubricated reference cylinder surface (0.23). It can be seen, that the friction coefficient of the ta-C + decoated cylinder was 0.16, which means about 30% below the untreated

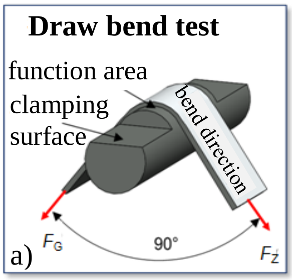

Rope friction
Eytelwein equation:

$$\mu = \frac{2}{\pi} \cdot ln\left(\frac{F_Z - F_B}{F_G}\right)$$

F_Z: Pulling Force
F_G: Back tension force
F_B: Bending force
b)

Fig. 6: Scheme of the draw bend test setup. a) The metal strip is bend around the function area of the tool by 90° and pulled back and forth. b) Rope friction formula to calculate the coefficient of friction during the bend test.

cylinder. A possible explanation is the highly increased value for surface roughness Sa of the coated + decoated surface (Tab. 1), which will be evaluated in future investigations.

The cylinder covered with the ta-C coating exhibited the lowest coefficient of friction (0.135), which is similar to the test results reported in [23]. This value is almost 40 % lower than for the uncoated surface.

An iteration of ta-C coating, decoating and repeated ta-C coating lead to an increase of the friction coefficient (0.16), what can be explained by the higher surface roughness of the ta-C surface. For the cylinders that were nitride before the ta-C deposition process, the measured friction coefficient was 0.145. This can be attributed to the low surface roughness after nitration and coating. The use of a N_2-atmosphere during the ta-C coating process lead to a friction coefficient of 0.155. The reason for this result can be explained by a lower sp^3-content in the ta-C film. The decrease of the sp^3-content could be attributed to the higher pressures that are used for nitrogen doping (which typically results in an increased sp^2-content).

Friction tests with DLIP structured ta-C coatings show a slight increase in the friction coefficient compared to unstructured ta-C surface. The draw-bend test of the coated and subsequently DLIP-structured tool shows a slightly increased friction coefficient (0.185) which is also similar as previous reported values [23]. This result can be linked to the modified sp^3/sp^2 ration at the interface maxima positions, where sp^2-rich elevations

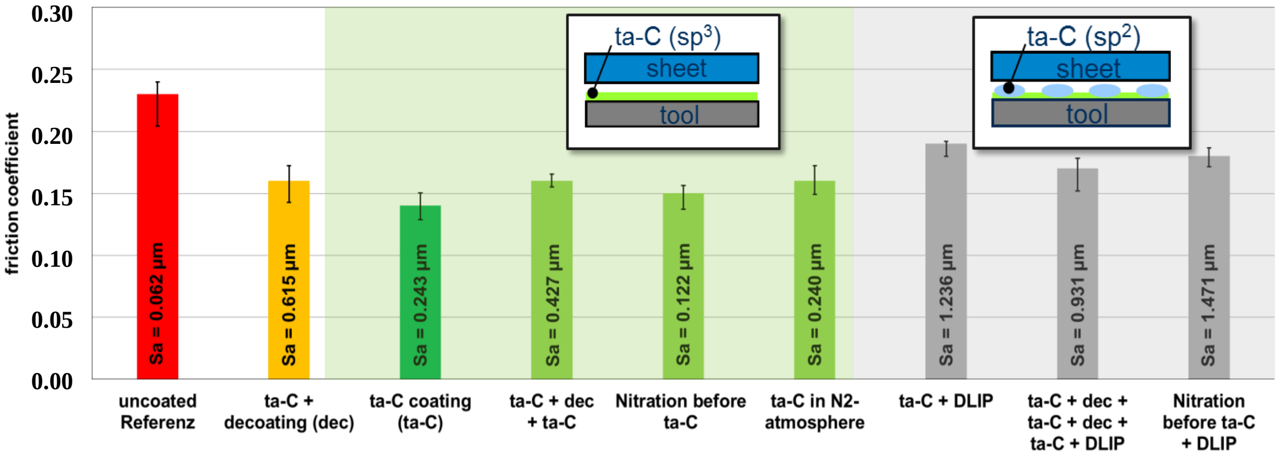

Fig. 7: Measured friction coefficients for coated and structured cylinders during draw bend test with DC04 stripes. The surface roughness parameter Sa is shown for better analysis of the dependencies.

change the contact geometry. The friction coefficient value of the cylinder with repetitive ta-C coating and decoating before the final ta-C structuring was slightly decreased (0.165) compared to the coated and structured sample (0.185). Although the friction coefficients for the laser treated samples increased compared to the ta-C coated samples, a significant reduction in the wear volume is expected, which will be evaluated in future investigations [23].

3 Summary and conclusion

In this paper, the tool optimization for dry forming applications was studied. Therefore, draw bend tools have been prepared by a variety of coating iterations of tetrahedral amorphous carbon films and subsequent DLIP micro-structuring. The surface roughness of the test cylinders was analysed before the draw bend tests. These results could be used to explain the different values of the friction coefficient measurement between the prepared test cylinders and draw-bend DC04 stripes. The lowest friction coefficient of 0.135 could be found for the cylinder with once ta-C coating without further structuring, compared to the highest friction coefficient of (0.23) for the untreated reference cylinder. This was in good agreement with previous test of this project group. Furthermore does the surface roughness of the steel cylinder as well as ta-C layer shows to influence the friction coefficient. The DLIP-structuring lead to a minor increase of the friction coefficient compared to the unstructured and coated tool. Cylinders with nitration before ta-C coating or ta-C coating during N_2-atmosphere were also tested, as ta-C modification, to study further their influence on the tribological performance.

Acknowledgements

The authors thank the project partners. Furthermore, the authors want to thank the German Research Foundation (DFG) for the financial support of the project “macro and micro structuring of deep drawing tools for dry forming” in priority program 1676 “Sustainable Production” by Dry Forming Technology. The work of Andrés Lasagni was partially supported by the German Research Foundation (DFG), Excellence Initiative by the German federal and state governments to promote top-level research at German universities (Grant No.: F-003661-553-71A-1132104).

References

[1] S. Kataoka, M. Murakawab, T. Aizawac, H. Iked: Tribology ofdry deep-drawing of various metal sheets with use of ceramics. Surface and Coatings Technology (2004) 177 –178 582–590
[2] K. Taube: Carbon-based coatings for dry sheet-metal working, Surface and Coatings Technology 1-3 (1998) 976-984
[3] K. Osakada, R. Matsumoto: Fundamental study of dry metal forming with coated tools, CIRP Annals-Manufacturing Technology (2000) 161-164
[4] V. Weihnacht, A. Brückner, S. Bräunling: ta-C beschichtete Werkzeuge für die Trockenumformung von Aluminiumblechen, Vakuum in Forschung und Praxis 20 (2008) 6-10
[5] F. Klocke, T. Maßmann, K. Gerschwiler: Combination of PVD tool coatings and biodegradable lubricants in metal forming and machining, Wear 259 (2005) 1197-1206
[6] P. Carlsson, M. Olsson: PVD coatings for sheet metal forming processes, a tribological evaluation, Surface and Coatings
[7] J. Robertson: Diamond-like amorphous carbon. Material Science and Engineering R37 (2002) 129
[8] A. Erdemir, C. Donnet: Tribology of diamond-like carbon films. J. Phys. D Appl. Phys. 39 (2006) R311–R327
[9] B. Schultrich: Modeling of ta-C growth: Influence of the technological parameters, Diam. Relat. Mater. 20 (2011) 785-792
[10] M. Murakawa, S. Takeuchi: Evaluation of tribological properties of DLC films used in sheet forming of aluminum sheet, Surface and Coatings Technology 163-164 (2003) 561-565
[11] B. Schultrich, V. Weihnacht: Tribologisches Verhalten von harten und superharten Kohlenstoffschichten, Vakuum in Forschung und Praxis 20 (2008) 12-17Technology 200 (2006) 4654-4663
[12] A. Mousavi, M. Schomäcker, A. Brosius: Macro and micro structuring of deep drawing’s tools for lubricant free forming, Procedia Engineering 81 (2014) 1890-1895
[13] T. Roch, V. Weihnacht, H.-J. Scheibe, A. Roch and A. F. Lasagni: Direct Laser Interference Patterning of tetrahedral carbon films for tribological applications, Diam. Relat. Mater. 33 (2013) 20-26
[14] T. Roch, D. Benke, S. Milles, T. Kunze and A. F. Lasagni: Dependence between friction of laser interference patterned carbon and the thin film morphology, Diam. Relat. Mater. 55 (2015) 16-21
[15] Y. Xia, G.M. Whitesides.: Soft lithography, Annual Review of Materials Science 28, (1998) p.153-184.
[16] M. Geissler, Y. Xia: Patterning: principles and some new developments, Advanced Materials 16, (2004) No. 15.
[17] F. Mücklich, A. Lasagni, C. Daniel: Laser interference metallurgy—periodic surface patterning and formation of intermetallics, Intermetallics 13, (2005) p. 437.
[18] L. Longstreth-Spoor, J. Trice, H. Garcia, C. Zhang, R. Kalyanaraman: Nanostructure and microstructure of laser-interference-induced dynamic patterning of Co on Si J. Phys. D: Appl. Phys. 39, (2006) p. 5149.
[19] M. K. Kelly, J. Rogg, C. E. Nebel, M. Stutzmann, S. Kátai: High-Resolution Thermal Processing of Semiconductors Using Pulsed-Laser Interference Patterning phys. stat. sol. (a) 166, (1998) p. 651.

[20] J Robertson: Diamond-like amorphous carbon, Materials Science and Engineering: R: Reports 37, Issue 4-6 (2002), 129-281.
[21] C. Donnet: Recent progress on the tribology of doped diamond-like and carbon alloy coatings: a review, Surface and Coating Technology, 100-101 (1998), 180-186.
[22] T. Jähnig, T. Roch, A. Lasagni: Development in dry metal forming – Structuring ta-C coated tools with direct laser interference patterning and ultra-short pulsed lasers to reduce friction and wear, Proceedings 38th International Congress on Applications of Laser & Electro-Optics, Oktober 2019, Orlando, Florida.
[23] T. Kunze, A. Mousavi, T. Stucky, F. Böttcher, T. Roch, M. Schomäcker, A. Lasagni, A. Brosius: Tool Optimization for Dry Forming Applications, THe "A" Coatings - 12th International Conference in Manufacturing Engineering, (2016) pp. 201-207.